Acta Crystallographica Section D
**Biological Crystallography**
ISSN 0907-4449

# Structure of an excitatory insect-specific toxin with an analgesic effect on mammals from the scorpion *Buthus martensii* Karsch

**Chong Li, Rong-Jin Guan, Ye Xiang, Ying Zhang and Da-Cheng Wang***

Center for Structural and Molecular Biology, Institute of Biophysics, Chinese Academy of Science, Beijing 100101, People's Republic of China

Correspondence e-mail: dcwang@sun5.ibp.ac.cn

Received 17 May 2004
Accepted 12 October 2004

**PDB Reference:** BmK IT-AP, 1t0z, r1t0zsf.

BmK IT-AP is an excitatory insect-specific $\beta$-toxin with analgesic effect from the Chinese scorpion *Buthus martensii* Karsch (BmK) and consists of 72 residues cross-linked by four disulfide bridges. The crystal structure of BmK IT-AP has been determined at a resolution of 2.6 Å by molecular replacement. Compared with the mammal-selective $\alpha$-toxins consisting of 64 residues from the scorpion BmK, the general fold of IT-AP features an additional one-and-a-half turn $\alpha$-helix at the C-terminal residues 59–65 with a shifted disulfide bridge Cys38–Cys64. The extension and 'wiggling' of the C-terminal segment led to a reshaping of the bioactive surface, including the complete destruction of the active site RC comprising the reverse turn (8–12) and C-terminal residues 58–64, the disappearance of an active surface formed by two aromatic residues Trp38 and Tyr42 and the covering of the conserved aromatic cluster Tyr5, Tyr35 and Trp47, which are all critical for the structure and function of mammal-selective $\alpha$-toxins. Bj-xtrIT, the only other excitatory insect-specific toxin whose three-dimensional structure has been determined, is distinct from BmK IT-AP. A functionally important five-residue $\alpha$-helix ($\alpha$0) formed by residues 17–21 in Bj-xtrIT is deleted in BmK IT-AP and helix $\alpha$1 is immediately connected to Cys16 through two residues Leu17 and Phe18. Accordingly, the functional surface of this region in Bj-xtrIT has also been reshaped in IT-AP, which implies subtle differences between BmK IT-AP and Bj-xtrIT in binding to the receptor, although most other critical residues for structure and function adopt almost identical conformations. The crystal structure of IT-AP also forms a sound basis for further study of the structure–function determinants of the analgesic effect.

## 1. Introduction

Scorpion toxins acting on voltage-dependent sodium channels in excitable cells are mainly related to human envenomation; they are classified as $\alpha$-toxins, which inhibit sodium-current inactivation, and $\beta$-toxins, which modify the activation process (Couraud *et al.*, 1982). Scorpion toxins exhibit high selectivity towards animals belonging to different phyla. They have been identified to act on mammals, insects and crustaceans with high specificity (Gordon *et al.*, 1998). The most intriguing property of scorpion toxins is that they can discriminate between insect and mammalian sodium channels. The highly insect-specific toxins are considered to belong to the $\beta$-toxins, as they compete with $\beta$-toxins for the same receptor-binding site (Gordon *et al.*, 1992). These insect toxins include two distinct subgroups: excitatory and depressant (Zlotkin *et al.*, 1971). Excitatory insect-specific toxins induce a sustained

contraction paralysis in fly larvae and shift insect $Na^+$-channel activation to a more negative membrane potential under voltage-clamp conditions (Zlotkin *et al.*, 1985; Pelhate & Zlotkin, 1982). Depressant insect toxins induce a slow depressant and flaccid paralysis preceded by a short transient phase of contracture. The anti-insect specificity of excitatory toxins has been used to study the properties of the sodium channel (Cestele *et al.*, 1997) in insects and in the development of a new insecticide (Stewart *et al.*, 1991; Gurevitz *et al.*, 1998).

Thus far, a series of excitatory insect-specific toxins have been purified and characterized (Zlotkin *et al.*, 1971; Kopeyan *et al.*, 1990; Ji *et al.*, 1996; Deena *et al.*, 1998; Xiong *et al.*, 1999, Cohen *et al.*, 2004), as shown in Fig. 1. These toxins are 70–76 amino-acid residues long with four highly conserved disulfide bridges, three of which are conserved in both $\alpha$- and $\beta$-toxins. Although a series of three-dimensional structures of scorpion mammal-specific toxins have been elucidated, only one crystal structure of an excitatory insect-specific toxin, Bj-xtrIT, has been reported to date (Deena *et al.*, 1998), mainly because of the difficulty in obtaining a sufficiently large quantity of highly pure and stable sample. Here, we report the crystal structure of a novel excitatory insect-specific toxin, BmK IT-AP, with an analgesic effect on mammals.

BmK IT-AP (insect toxin analgesic protein) was purified from the venom of the scorpion *Buthus martensii* Karsch (BmK), which is widely distributed in China and East Asia. BmK IT-AP displays typical excitatory insect-selective toxicity. Interestingly, BmK IT-AP also exhibits an analgesic effect, but is devoid of any toxicity to mice (Xiong *et al.*, 1999). The bioassay showed that its analgesic effect was not parallel to the insect toxicity, which suggested a distinct structure–function determinant for the analgesic effect (Guan *et al.*, 2000). BmK IT-AP consists of 72 amino-acid residues cross-linked by four disulfide bridges and is homologous to all other excitatory insect-specific toxins with sequence identity of 75–82%, except for Bj-xtrIT. BmK IT-AP has a sequence identity of 62% with Bj-xtrIT and differs remarkably in the deletion of a five-residue motif (17–21) after the first cysteine (Cys16) (Fig. 1), which has been identified to be part of the toxin-receptor binding site (Cohen *et al.*, 2004). Thus, BmK IT-AP should be considered as a representative of the subtype of excitatory insect toxins with 72 amino-acid residues. The three-dimensional structure of BmK IT-AP will expand our structural knowledge of the excitatory insect-specific toxins and form a sound structural basis for understanding its dual bioactivity: namely, its toxicity to insects and its analgesic effect on mammals.

Furthermore, a series of crystal structures of toxins from the scorpion BmK, including BmK M1, M2, M4, M7 and M8 (PDB codes 1sn1, 1chz, 1sn4, 1kv0 and 1snb, respectively; Li *et al.*, 1996; He *et al.*, 1999, 2000; Guan *et al.*, 2004), have been determined, all of which belong to the $\alpha$-toxins. BmK M1 is highly mammal-selective and has been the subject of extensive analysis by mutagenesis in order to identify the important sites

**Table 1**
Data-collection and structural refinement statistics.

Values in parentheses are for the highest resolution shell.

| | |
|---|---|
| Data collection | |
| Total reflections | 136909 |
| Unique reflections | 7244 |
| Resolution range (Å) | 500–2.60 |
| Completeness (%) | 100 (100) |
| Average $I/\sigma(I)$ | 28.5 (7.2) |
| $R_{merge}$ (%) | 7.1 (30.3) |
| Asymmetric unit contents | 2 molecules |
| Structure refinement | |
| $R_{work}$ | 0.200 |
| $R_{free}$ | 0.249 |
| No. non-H atoms | 1246 |
| Protein | 1136 |
| Sulfate ions | 55 |
| Waters | 65 |
| Average temperature factor (Å$^2$) | |
| Protein | 27.2 (mol. *A*), 34.9 (mol. *B*) |
| Main chain | 26.8 (mol. *A*), 33.8 (mol. *B*) |
| Side chain | 27.6 (mol. *A*), 36.0 (mol. *B*) |
| Waters | 38.6 |
| Sulfate ions | 48.9 |
| R.m.s.d from standard stereochemistry | |
| Bond length (Å) | 0.008 |
| Bond angles (°) | 1.30 |
| Dihedral angles (°) | 21.80 |
| Improper (°) | 0.79 |
| Ramachadran plot, residues in | |
| Core region (%) | 89.2 (mol. *A*), 90.8 (mol. *B*) |
| Allowed region (%) | 10.8 (mol. *A*), 9.2 (mol. *B*) |

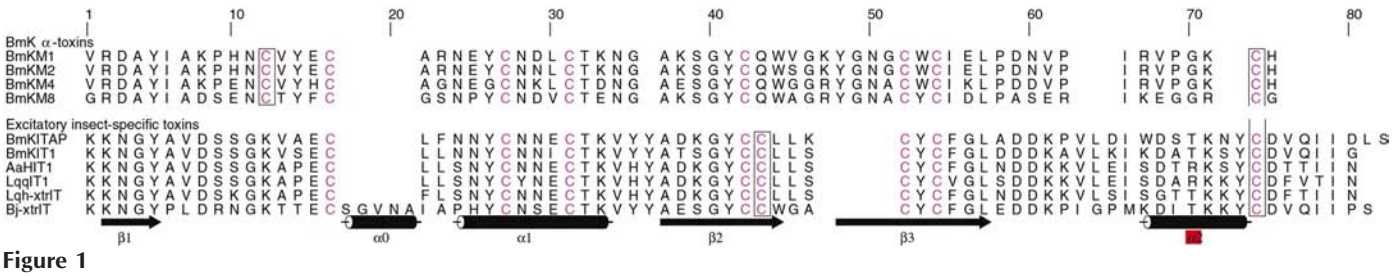


**Figure 1**
Sequence alignments of BmK IT-AP with BmK $\alpha$-toxins and other scorpion excitatory insect toxins. Conserved secondary-structural elements are shown, of which helix $\alpha$2 is unique to excitatory insect-specific toxins. Sequences are aligned according to the cysteine frame. The cysteine (highlighted with box in blank background) cross-linked to the last cysteine in the sequence is dramatically shifted from position 12 in $\alpha$-toxins to position 38 in BmK IT-AP and in all excitatory insect toxins. AaHIT1 and AaHII are from the scorpion *Androctonus australis* Hector, LqqIT1 is from scorpion *Leiurus quinquestriatus quinquestriatus*, Lqh-xtrIT is from the scorpion *L. quinquestriatus hebraeus* and Bj-xtrIT is from the scorpion *Buthotus judaicus* (Possani *et al.*, 1999; Deena *et al.*, 1998; Cohen *et al.*, 2004). BmK M1, M2, M4, M8, IT-AP and IT1 are from the scorpion *B. martensi* Karsch (He *et al.*, 1999; Li *et al.*, 1996; Luo *et al.*, 1997; Xiong *et al.*, 1999).

for structure and function (Wang *et al.*, 2003; Sun *et al.*, 2002, 2003). The structure of BmK IT-AP as an insect-specific $\beta$-toxin in comparison with BmK M1 as a mammal-selective $\alpha$-toxin will reveal the structural determinants that discriminate these two phylogenetically distinct scorpion toxins.

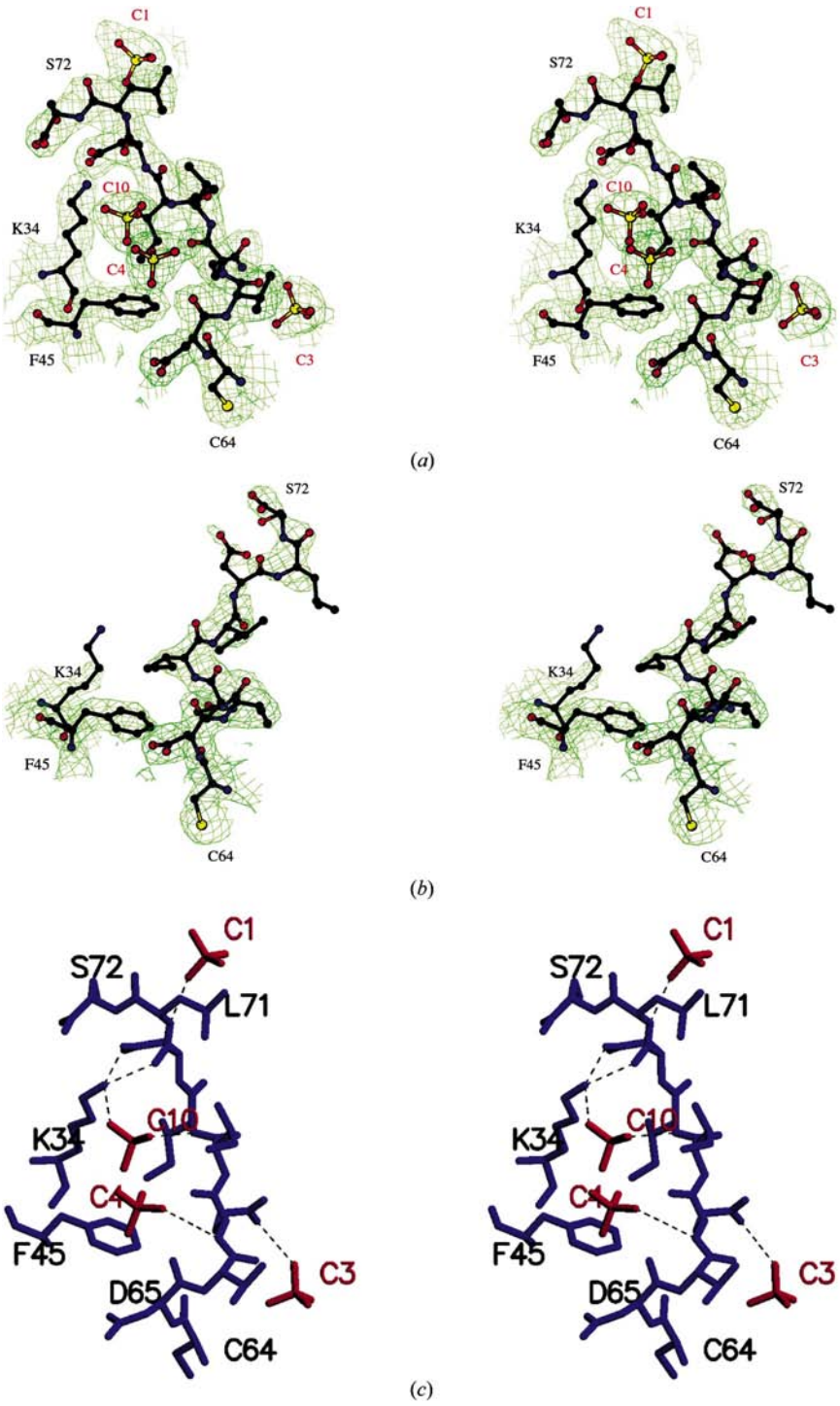


**Figure 2**
Stereoview of the C-terminal segments of BmK IT-AP showing the different conformational states of the C-tail of the two molecules in the asymmetric unit. (*a*) Molecule *A*, (*b*) molecule *B*. The electron-density maps ($2F_o - F_c$, contoured at $1.0\sigma$) also show the four well defined sulfate ions (C1, C3, C4 and C10) stabilizing the conformation of molecule *A*. (*c*) The interaction between the C-terminus of molecule *A* and the sulfate ions, highlighted in red.

## 2. Materials and methods

### 2.1. Purification and crystallization

BmK IT-AP was purified from the crude venom of BmK as described by Xiong *et al.* (1999). BmK IT-AP was crystallized at 287 K by the hanging-drop vapour-diffusion method. The hanging drop consisted of 2 µl 20 mg ml$^{-1}$ BmK IT-AP dissolved in 1 m*M* acetic acid mixed with 2 µl reservoir solution [1.4 *M* $(NH_4)_2SO_4$ and 0.1 *M* CHES pH 9.5] and 0.6 µl 4 m*M* Zwittergent 3-10. The drops were left to equilibrate against 600 µl reservoir solution. Within one week, crystals grew to dimensions of 0.3 × 0.15 × 0.15 mm (Guan *et al.*, 2000).

Preliminary crystallographic analysis showed that the crystal belongs to space group $P6_422$ or $P6_222$, with unit-cell parameters $a = b = 64.97$, $c = 173.48$ Å. There are two molecules in the asymmetric unit and the solvent content is estimated to be 60.5% according to the Matthews coefficient ($V_M = 3.11$ Å$^3$ Da$^{-1}$; Matthews, 1968).

### 2.2. Data collection and processing

The diffraction data of BmK IT-AP were collected with wavelength 1.0 Å at room temperature on beamline BL-18B at the Photon Factory, KEK, Tsukuba, Japan using an ADSC Q4R CCD detector. A complete data set to 2.6 Å resolution was integrated, scaled and merged using the *HKL* package (Otwinowski & Minor, 1997). The final data-collection statistics are listed in Table 1.

### 2.3. Molecular replacement

The structure of BmK IT-AP was solved by the molecular-replacement method using *MOLREP* v.7.3 (Vagin & Teplyakov, 1997) from the *CCP*4 v.4.2 software suite (Collaborative Computational Project, Number 4, 1994). The crystal structure of Bj-xtrIT (PDB code 1bcg) was used as a search model. No atoms were substituted or omitted from the model. Both space group $P6_422$ and $P6_222$ were used in molecular replacement in the resolution range 29.53–3.0 Å. When $P6_422$ was used, the best solution calculated by the rotation function gave a correlation coefficient of 30.0% with an *R* factor of 56.7% and the subsequent translation function gave a clear solution of two molecules in the asymmetric unit with a correlation coefficient of 43.6% and an *R* factor of 51.1%. When $P6_222$ was used, the rotation and translation function gave a

correlation coefficient of only 22.6% with an $R$ factor of 61.0% and a correlation coefficient of 26.8% with an $R$ factor of 60.0%, respectively. This solution was confirmed by checking the packing using the program *O* (Jones *et al.*, 1991).

### 2.4. Model building and refinement

The model was rebuilt using *O* and refined with the program *CNS* (Brünger *et al.*, 1998). 10% of the unique reflections were selected randomly to calculate the free $R$ factor (Kleywegt & Brünger, 1996). Following rigid-body refinement, several rounds of simulated-annealing refinement were performed alternating with the calculation of electron-density maps and manual adjustment of the model. Positional and individual $B$ factors were then refined and solvent molecules were identified and added to the model. Some electron densities, which were clearly greater than water molecules in the $2F_o - F_c$ and $F_o - F_c$ maps, were defined as sulfate ions. Finally, energy-minimization refinement with *CNS* was carried out, followed by restrained refinement with *REFMAC*5 (Murshudov *et al.*, 1999) in the final round to further improve the accuracy of the model. The final model, including 1136 protein atoms, 65 water molecules and 11 sulfate ions, was refined to $R_{work}$ = 20.0% ($R_{free}$ = 24.9%) in the resolution range 29.53–2.6 Å. The final structure was analyzed using *PROCHECK* (Laskowski *et al.*, 1993).

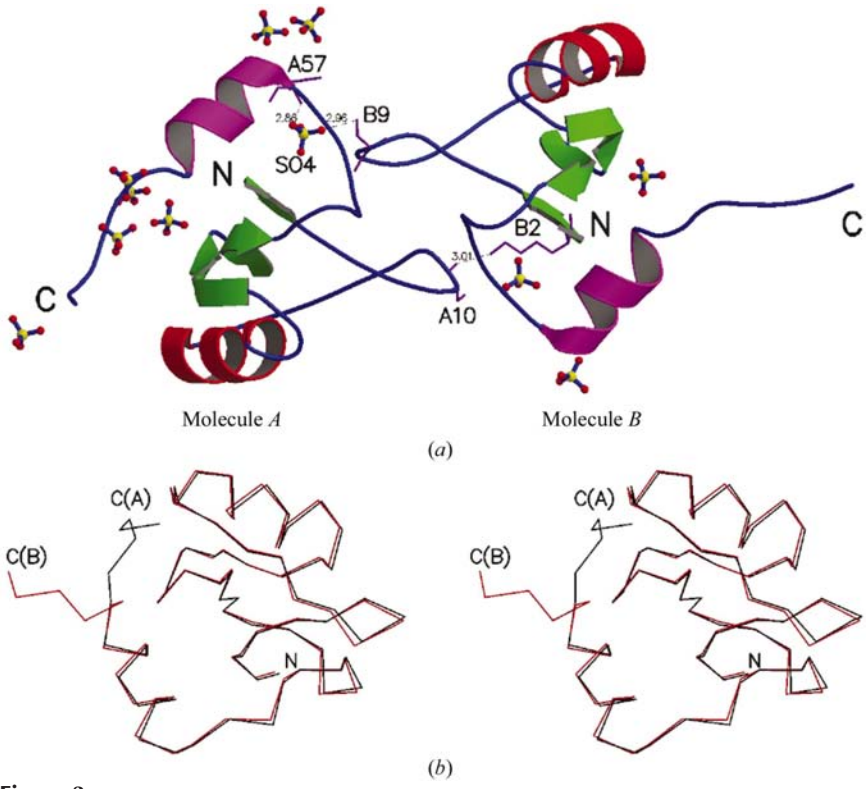


**Figure 3**
General structure of BmK IT-AP. (*a*) Crystallographic dimer of IT-AP in the asymmetric unit and the monomer–monomer interactions. The three hydrogen bonds are shown as broken lines. 11 sulfate ions are shown as ball-and-stick models: seven around molecule *A*, three around molecule *B* and one mediating molecule *A*–molecule *B* contacts. (*b*) Superposition of $C^{\alpha}$ atoms of molecule *A* (black) and molecule *B* (red). The six flexible C-terminal residues adopt different conformations in molecule *A* and molecule *B*.

## 3. Results and discussion

### 3.1. Quality of the structure

The two molecules, molecule *A* and molecule *B*, in the asymmetric unit were well refined and the refinement statistics are given in Table 1. Each molecule contains all 72 amino-acid residues. The Ramachandran plot (Ramachandran & Sasisekharan, 1968) reveals that 89.2 and 90.8% of the non-glycine and non-proline residues of molecules *A* and *B*, respectively, fall in the core region; the remainder are all in the allowed region.

Since the C-terminal stretch 67–72 in molecule *B* is flexible (Fig. 2), the average $B$ factor of molecule *B* (34.9 Å$^2$) is significantly higher than that of molecule *A* (27.2 Å$^2$). Except for the last six residues of molecule *B*, all residues are well defined in the electron-density maps. 11 sulfate ions can be identified in $2F_o - F_c$ and $F_o - F_c$ maps; they mainly contribute to the monomer–monomer interactions and stabilization of the C-terminal segment of molecule *A* (Figs. 2 and 3).

### 3.2. Overall structure of BmK IT-AP

The two molecules, *A* and *B*, in the asymmetric unit are related by a non-crystallographic twofold axis. They interact with each other through three hydrogen bonds, including a direct hydrogen bond (*A*10 O$\cdots$*B*2 NZ, 3.01 Å) and two sulfate-mediated contacts (Fig. 3). Superposition of molecules *A* and *B* shows that except for the C-terminal four residues, their conformations are very similar and the root-mean-square deviation of $C^{\alpha}$ atoms from residues 1–68 is 0.45 Å (Koradi *et al.*, 1996). The C-terminal stretches 68–72 of these two molecules are in different conformational states: rigid in molecule *A* but flexible in molecule *B* (Fig. 3). Since the defined conformations of the C-terminal residues 68–72 are mainly stabilized by five sulfate ions in the crystal, the C-terminal segment of IT-AP should be in a flexible state in solution.

The general fold of IT-AP revealed by the crystal structure can be described as consisting of two parts: the N-sector (residues 1–59) and the C-lobe (residues 60–72) (Fig. 3). The N-sector has the same $\beta\alpha\beta\beta$ motif as in $\alpha$-toxins (Fig. 4). It is composed of a dense core of secondary-structure elements, including an $\alpha$-helix formed by residues 19–28 and a three-stranded antiparallel $\beta$-sheet formed by residues 2–5, 32–38 and 45–54. Three disulfide bridges formed by Cys16–Cys37, Cys22–Cys42 and Cys26–Cys44 stabilize this special motif; they are strictly conserved in all scorpion $\alpha$-toxins and $\beta$-toxins. Compared with the $\alpha$-toxins, the only structural change in this part is that loop 38–44, which was identified to be of functional importance in $\alpha$-toxins

(Sun *et al.*, 2003), is deleted in the sequence of IT-AP (Figs. 1 and 4). However, the C-lobe (residues 60–72) of IT-AP is strikingly different from that in $\alpha$-toxins; it features an additional one-and-a-half turn $\alpha$-helix ($\alpha$2) formed by residues 59–65 and a disulfide bridge Cys38–Cys64 that is shifted from the fourth disulfide bond Cys12–Cys63 of $\alpha$-toxins (Fig. 4). These new structural elements give IT-AP a molecular framework and topology distinct from that of $\alpha$-toxins.

### 3.3. Main structural disparity between BmK IT-AP and BmK $\alpha$-toxins

In all $\alpha$-toxins a five-residue reverse turn (8–12) at the N-terminus connects with the C-terminal segment 58–64 to form a unique tertiary structure (Fig. 4), which is anchored to the $\beta\alpha\beta\beta$ molecular scaffold through a complicated hydrogen-bonding network and the fourth disulfide bond Cys12–Cys63. This unique local structure has been called site RC (He *et al.*, 1999; Wang *et al.*, 2003). Site-directed mutagenesis investigations of BmK M1 have identified site RC as being crucial for the structure and function of the toxin (Wang *et al.*, 2003; Sun *et al.*, 2002). Residues Asn11, Arg58 and Cys12 and Cys63 of the disulfide bridge have been shown to be responsible for stabilizing the unique conformation of this functional site. Mutating any one of them seriously reduced the bioactivity of the toxin and synchronously altered the conformation (Wang *et al.*, 2003; Sun *et al.*, 2002). In fact, in all $\alpha$-toxins Asn11 provides side-chain atoms $O^{\delta1}$ and $N^{\delta2}$ to connect the main chain of Val59 through 11 $O^{\delta1}\cdots$59 N and 11 $N^{\delta2}\cdots$59 O hydrogen bonds (Fig. 4). In addition, the carbonyl O atom of Asn11 makes a hydrogen bond with Arg58 $N^{\varepsilon}$, which is further connected to Gly61 *via* a hydrogen bond. Correspondingly, Asn11 and Cys12 are strictly conserved and residue 58 is conserved as Arg or Lys in all $\alpha$-toxins (Cestele *et al.*, 1999). Furthermore, mutagenesis analysis (Sun *et al.*, 2002) has shown that the disulfide bond Cys12–Cys63 is only critical for stabilizing the local structure relevant to the C-tail in BmK M1, not for the general folding of M1. In the structure of IT-AP, residue 11 is changed to Gly from Asn (Fig. 1) and all the interactions described above in the $\alpha$-toxins are lost. Additionally, the fourth disulfide bridge is shifted from 12–63 to a new position 38–64 to connect the lengthened C-terminal segment to the molecular scaffold with a new pattern (Fig. 4). It seems that the change of residue 11 from Asn to Gly is a critical structural factor for switching on the unique C-tail conformation of BmK IT-AP.

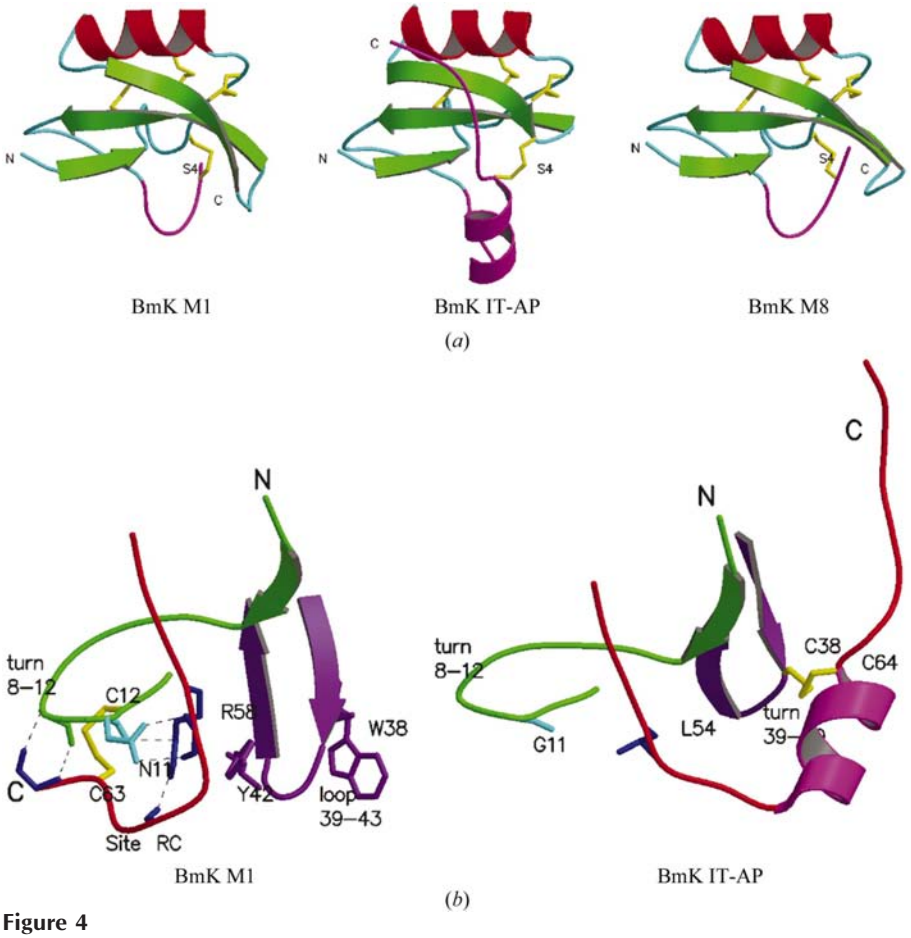


**Figure 4**
Comparison of BmK IT-AP and BmK $\alpha$-toxins ($\alpha$-like toxin M1 and classic $\alpha$-toxin M8). (*a*) Overall structures of BmK IT-AP, M1 (He *et al.*, 1999) and M8 (Li *et al.*, 1996). C-termini are shown in magenta, where IT-AP forms a unique helix distinct from those of M1 and M8. Three conserved disulfide bridges and the shifted disulfide bridge (S4) are highlighted in yellow. The conserved common structure motif $\beta\alpha\beta\beta$ is shown in red and green. (*b*) The local structures of the reverse turn 8–12 (RT) and the C-terminal segment (CT) in BmK M1 and in IT-AP, showing some of the structural factors that trigger the unique C-terminal conformation of BmK IT-AP. In M1 the turn 8–12 connects the C-terminus 58–64 *via* a hydrogen-bonding network in which Asn11 plays a critical role to form a unique tertiary arrangement (site RC). In IT-AP the network is absent; Asn11 in M1 is mutated to Gly11 in IT-AP, the disulfide bridge Cys12–Cys63 in M1 is shifted to Cys38–Cys64 and the orientation of the C-terminus is dramatically changed to be distant from the turn 8–12.

Site-directed mutagenesis of BmK M1 also suggested that $\alpha$-toxins have two bioactive surfaces which may directly interact with the receptor site on the sodium channel. One is located in site RC and mainly consists of the C-terminal basic residues Lys62 and His64 (Wang *et al.*, 2003). Another one involves two conserved aromatic residues Trp38 and Tyr42 on the loop 38–44 between $\beta$2 and $\beta$3, called site AR (Sun *et al.*, 2003). In BmK IT-AP the first active surface has clearly been changed. The hydrogen-bonding network between the turn 8–12 and the C-terminus in site RC of BmK M1 have been destroyed completely in IT-AP (Fig. 4), so the surface of IT-AP in this region differs distinctly from that of M1 (Fig. 5). Furthermore, in IT-AP the residues corresponding to residues

41–45 of the $\alpha$-toxins have been deleted and Trp38 has changed to Leu, which leads to the disappearance of another active surface site AR in $\alpha$-toxins (Figs. 4 and 5).

Furthermore, in all $\alpha$-toxins there is a conserved aromatic residue cluster, Tyr5, Tyr35 and Trp47, apparent on the so-called the conserved hydrophobic surface (CHS), which is assumed to be part of the functional site targeting the sodium channel (Fontecilla-Camps *et al.*, 1988; Li *et al.*, 1996). Detailed mutagenesis analysis of these three aromatic residues has shown that they contribute to the function of the toxin mainly through stabilizing the three-stranded $\beta$-sheet (Sun *et al.*, 2003). In the IT-AP structure, this aromatic cluster still exists, but it is covered by the lengthened C-terminal segment (Fig. 5). This indicates that this conserved aromatic residue cluster, while still able to stabilize the molecular scaffold in BmK IT-AP, is not involved in interaction with the receptor.

Evidently, although the $\alpha$-toxins and $\beta$-toxins possess the same molecular scaffold in the N-terminal part, the extension and 'wiggling' of the C-terminal segment of BmK IT-AP have led to reshaping of the bioactive surface and a different topology of the molecule; this forms the main structural basis for the insect-specific bioactivity of BmK IT-AP. It is plausible to infer that the functional site of IT-AP will be completely different from that of $\alpha$-toxins.

### 3.4. Comparison of BmK IT-AP with Bj-xtrIT

The only other crystal structure of an excitatory insect-specific toxin determined to date is that of Bj-xtrIT from the scorpion *Butholus judaicus* (Deena *et al.*, 1998). Bj-xtrIT shares 44–62% sequence identity with other excitatory toxins found so far, including BmK IT-AP, and differs remarkably from the others, with an insertion of five residues (17–21) after the first cysteine (Cys16). The superimposed main chains of BmK IT-AP and Bj-xtrIT (Fig. 6) show that the N-terminal motif and the additional helix $\alpha$2 in the C-terminal part are similar in the two toxins. The major differences between BmK IT-AP and Bj-xtrIT occur at the five-residue insertion (17–21, numbering as inBj-xtrIT) (Fig. 1) after the first conserved cysteine (Cys16) and prior to the first helix $\alpha$1. The crystal structure of Bj-xtrIT showed that these inserted residues formed a short $\alpha$-helix ($\alpha$0) on the molecular surface. More recently, site-directed mutagenesis has identified the solvent-exposed region formed by these residues as part of the surface of Bj-xtrIT that interacts with its receptor site (Cohen *et al.*, 2004). In the BmK IT-AP structure, this short helix ($\alpha$0) is absent and helix $\alpha$1 is directly connected to Cys16 through two residues Leu17 and Phe18 (numbering as in BmK IT-AP). Accordingly, the functional surface in this region of Bj-xtrIT has also been reshaped in IT-AP (Fig. 6). Therefore, it is plausible to infer that the property of binding to the receptor site on the sodium channels may be subtlely different between BmK IT-AP and Bj-xtrIT. Therefore, the structures of BmK IT-AP and Bj-xtrIT could be considered as representative

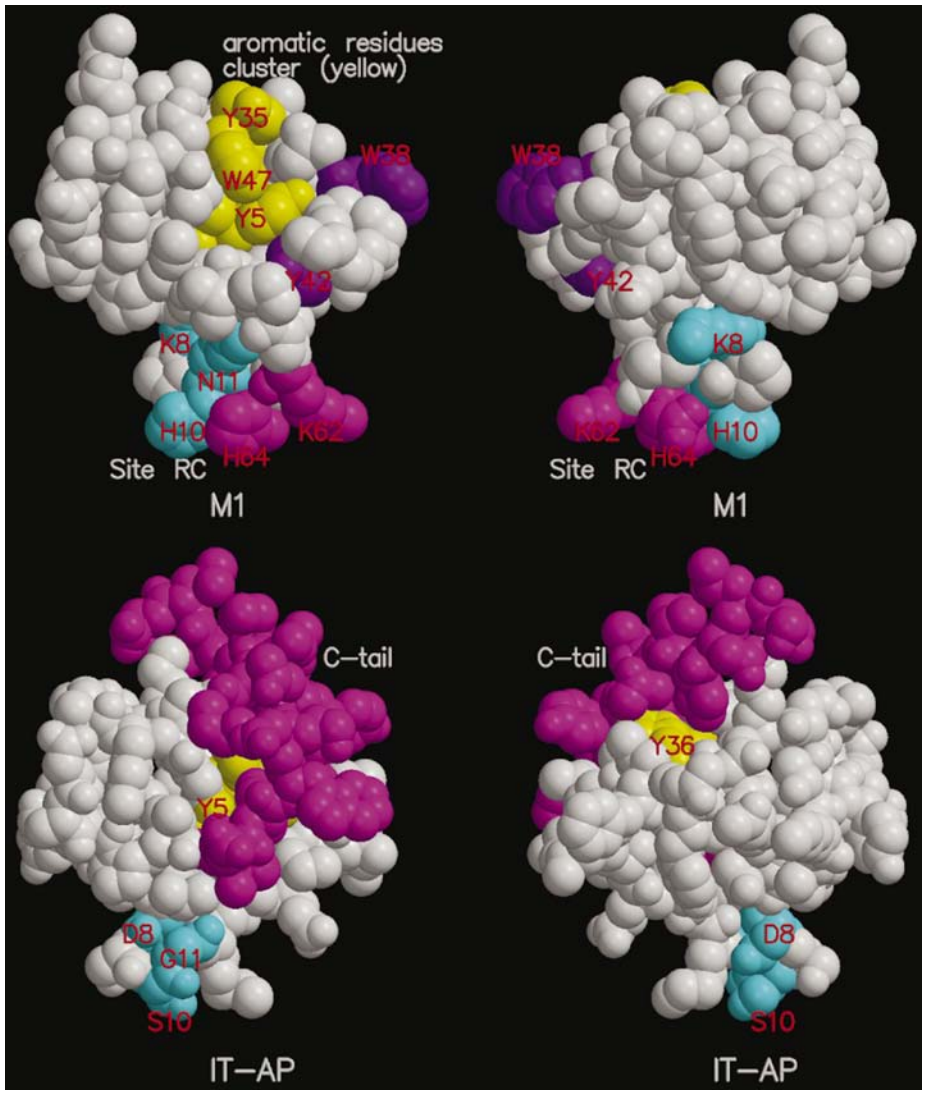


**Figure 5**
The functionally important surfaces of BmK M1 (top) and their reshaping in BmK IT-AP (bottom). The change in direction of the C-tail (magenta) of IT-AP compared with M1 destroys the structurally and functionally important site RC (cyan and magenta) of M1 and the cluster of conserved aromatic residues (Tyr5, Tyr35 and Trp47, yellow) of M1 is buried in IT-AP. Meanwhile, the surface formed mainly by the positively charged residues Lys62 and His64 of M1 and crucial in interaction with the $Na^+$ channel is absent in IT-AP. The two aromatic residues (Trp38 and Tyr42, purple) critical for pharmacological activity of BmK M1 are also absent in IT-AP. The molecules on the right are related to those on the the left by a rotation of 180° around the vertical axis.

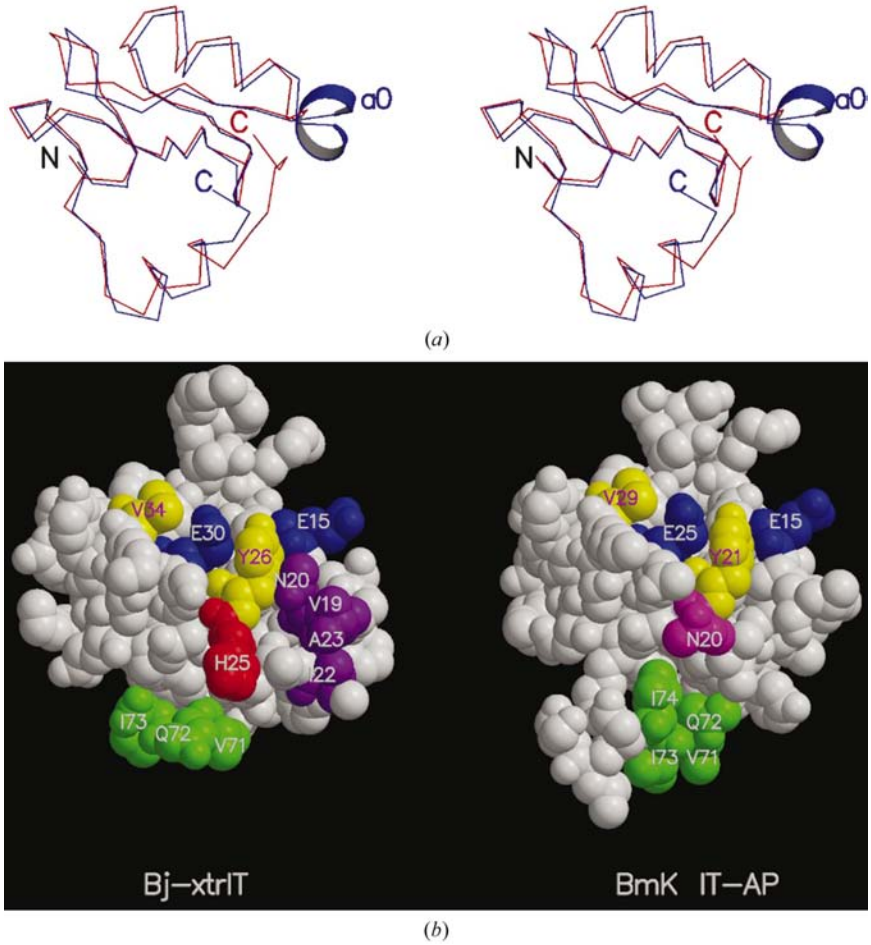


**Figure 6**
Comparisons of BmK IT-AP and Bj-xtrIT. (*a*) Comparison of the $C^{\alpha}$ traces of IT-AP (red) and Bj-xtrIT (blue), showing that the short $\alpha$-helix ($\alpha$0) formed by the additional five residues (17–21) of Bj-xtrIT is absent in IT-AP. (*b*) Surfaces of Bj-xtrIT important for function (left) and their corresponding positions in BmK IT-AP (right). The solvent-exposed surface (purple) consisting of residues Val19, Asn20, Ile22 and Ala23 in Bj-xtrIT is absent in IT-AP, as helix $\alpha$0 is not present in Bj-xtrIT. The residues Glu15, Tyr26, Glu30, Val34 and Val71-Gln72-Ile73-Ile74 (green) involved in the functionally important surfaces (Cohen *et al.*, 2004) are conformationally conserved in IT-AP; another important residue His25 of Bj-xtrIT has been mutated to Asn20 in IT-AP. The model of Bj-xtrIT is built from coordinates from the PDB (ID code 1bcg; Deena *et al.*, 1998).

models of two subtypes of the excitatory insect-specific toxins.

Dissection of the functional sites of Bj-xtrIT by mutagenesis has also suggested that two residue clusters constitute the main functional surface of the toxin (Cohen *et al.*, 2004). One cluster appears in helix $\alpha$1 and its vicinity, including Glu15, Glu30, Tyr26 and Val34, and the other cluster in the C-terminal region, including Val71, Gln72, Ile73 and Ile74 (Fig. 6). These residues invariably appear at the corresponding positions of BmK IT-AP. The structural comparison indicates that residues Glu15, Glu30, Tyr26 and Val34 adopt almost identical conformations in both IT-AP and Bj-xtrIT (Fig. 6). The residue cluster at the C-terminal region showed some conformational difference between the two toxins. However, the C-terminal segments also displayed distinct conformational states for molecules *A* and *B* in the asymmetric unit owing to different environments in the crystal, as described above. It seems that the flexibility of the C-terminal stretch is intrinsic. Thus, the conformational difference of the C-terminal segments observed in BmK IT-AP and Bj-xtrIT may not have biological significance.

### 3.5. Analgesic effect of BmK IT-AP

Two excitatory insect toxins, IT-AP and AngP1 (Xiong *et al.*, 1999; Guan *et al.*, 2001), from the venom of the scorpion BmK have been found to produce an analgesic effect on mice. However, the mechanism by which these toxins modulate the sensation of pain remains to be clarified. Evidently, the analgesic effect of IT-AP and AngP1 cannot be ascribed to any mammalian neurotoxicity the peptides may possess, as they have no detectable toxicity to mice. In fact, the present structure of IT-AP showed that all the functional sites of the BmK toxins specific to mammals have been changed in IT-AP, as described above. Additionally, a bioassay indicated that the analgesic effect of IT-AP on mice is at least 4–5 times stronger than that of AngP1, but its toxicity to insects is two times weaker than that of AngP1 (Guan *et al.*, 2001). Evidently, the analgesic effects of these peptides are not parallel to the insect toxicity. Thus, it seems that IT-AP and AngP1 may have unique structure–function determinants responsible for the analgesic effect that are distinct from those for the insect-specific effects. The crystal structure of BmK IT-AP forms a sound basis for further study on the structural mechanism of the analgesic effects of IT-AP.

This work was supported by the NNSF (30370320), the MOST (973-G1999075064 and 863-2002BA711A13) of China and the Chinese Academy of Sciences (KSCX1-SW-17). We thank the KEK for providing beam time at the Photon Factory for the X-ray experiment (2002 G310) and Professor N. Sakabe for his help in data collection.

## References

Brünger, A. T., Adams, P. D., Clore, G. M., DeLano, W. L., Gros, P., Grosse-Kunstleve, R. W., Jiang, J.-S., Kuszewski, J., Nilges, M., Pannu, N. S., Read, R. J., Rice, L. M., Simonson, T. & Warren, G. L. (1998). *Acta Cryst.* D**54**, 905–921.
Cestele, S., Gordon, D., Kopeyan, C. & Rochat, H. (1997). *Insect Biochem. Mol. Biol.* **27**, 523–528.
Cestele, S., Stankiewicz, M., Mansuelle, P., De Waard, M., Dargent, B., Gilles, N., Pelhate, M., Rochat, H., Martin-Eauclaire, M. F. & Gordon, D. (1999). *Eur. J. Neurosci.* **11**, 975–985.

Cohen, L., Karbat, I., Gilles, N., Froy, O., Corzo, G., Angelovici, R., Gordon, D. & Gurevitz, M. (2004). *J. Biol. Chem.* **279**, 8206–8211.
Collaborative Computational Project, Number 4 (1994). *Acta Cryst.* D**50**, 760–763.
Couraud, F., Jover, E., Dubois, J. M. & Rochat, H. (1982). *Toxicon*, **20**, 9–16.
Deena, A. O., Oren, F., Efrat, A., Nurit, K., Michael, G. & Boaz, S. (1998). *Structure*, **6**, 1095–1103.
Fontecilla-Camps, J. C., Habersetzer-Rochat, C. & Rochat, H. (1988). *Proc. Natl Acad. Sci. USA*, **85**, 7443–7447.
Gordon, D., Moskowitz, H., Eitan, M., Warner, C., Catterall, W. A. & Zlotkin, E. (1992). *Biochemistry*, **31**, 7622–7628.
Gordon, D., Savarin, P., Gurevitz, M. & Zinn-Justin, S. (1998). *J. Toxicol. Toxin Rev.* **17**, 131–159.
Guan, R.-J., Liu, X. Q., Liu, B., Wang, M. & Wang, D.-C. (2000). *Acta Cryst.* D**56**, 1012–1014.
Guan, R.-J., Wang, C. G., Wang, M. & Wang, D.-C. (2001). *Biochim. Biophys. Acta*, **1549**, 9–18.
Guan, R.-J., Xiang, Y., He, X. L., Wang, C. G., Wang, M., Zhang, Y., Sundberg, J. & Wang, D.-C. (2004). *J. Mol. Biol.* **341**, 1189–1204.
Gurevitz, M., Froy, O., Zilberberg, N., Turkov, M., Strugatsky, D., Gershburg, E., Lee, D., Adams, M. E., Tugarinov, V., Anglister, J., Shaanan, B., Loret, E., Stankiewicz, M., Pelhate, M., Gordon, D. & Chejanovsky, N. (1998). *Toxicon*, **36**, 1671–1682.
He, X. L., Li, H. M., Zeng, Z. H., Liu, X. Q., Wang, M. & Wang, D.-C. (1999). *J. Mol. Biol.* **292**, 125–135.
He, X. L., Deng, J. P., Wang, M., Zhang, Y. & Wang, D. C. (2000). *Acta Cryst.* D**56**, 25–33.
Ji, Y. H., Mansuelle, P., Terakawa, S., Kopeyan, C., Yanaihara, N., Hsu, K. & Rochat, H. (1996). *Toxicon*, **34**, 987–1001.
Jones, T. A., Zou, J. Y., Cowan, S. W. & Kjeldgaard, M. (1991). *Acta Cryst.* A**47**, 110–119.
Kleywegt, G. J. & Brünger, A. T. (1996). *Structure*, **4**, 897–904.
Kopeyan, C., Mansuelle, P., Sampieri, F., Brando, T., Bahraoui, E. M., Rochat, H. & Granier, C. (1990). *FEBS Lett.* **261**, 423–426.
Koradi, R., Billeter, M. & Wuthrich, K. (1996). *J. Mol. Graph.* **14**, 51–32.
Laskowski, R. A., MacArthur, M. W., Moss, D. S. & Thornton, J. M. (1993). *J. Appl. Cryst.* **26**, 283–291.
Li, H. M., Wang, D. -C., Zeng, Z. H., Jin, L. & Hu, R. Q. (1996). *J. Mol. Biol.* **261**, 415–431.
Luo, M. J., Xiong, Y. M., Wang, M., Wang, D.-C. & Chi, C. W. (1997). *Toxicon*, **35**, 723–731.
Matthews, B. W. (1968). *J. Mol. Biol.* **33**, 491–497.
Murshudov, G. N., Vagin, A. A., Lebedev, A., Wilson, K. S. & Dodson, E. J. (1999). *Acta Cryst.* D**55**, 247–255.
Otwinowski, Z. & Minor, W. (1997). *Methods Enzymol.* **276**, 307–326.
Pelhate, M. & Zlotkin, E. (1982). *J. Exp. Biol.* **97**, 67–77.
Possani, L. D., Becerril, B., Delepierre, M. & Tytgat, J. (1999). *Eur. J. Biochem.* **264**, 287–300.
Ramachandran, G. N. & Sasisekharan, V. (1968). *Adv. Protein Chem.* **23**, 283–438.
Stewart, L. M., Hirst, M., Lopez, F. M., Merryweather, A. T., Cayley, P. J. & Possee, R. D. (1991). *Nature (London)*, **352**, 85–88.
Sun, Y. M., Bosmans, F., Zhu, R. H., Goudet, C., Xiong, Y. M., Tytgat, J. & Wang, D.-C. (2003). *J. Biol. Chem.* **278**, 24125–24131.
Sun, Y. M., Liu, W., Zhu, R. H., Goudet, C., Tytgat, J. & Wang, D.-C. (2002). *J. Pept. Res.* **60**, 247–256.
Vagin, A. & Teplyakov, A. (1997). *J. Appl. Cryst.* **30**, 1022–1025.
Wang, C. G., Gilles, N., Hamon, A., Le Gall, F., Stankiewicz, M., Pelhate, M., Xiong, Y. M., Wang, D.-C. & Chi, C. W. (2003). *Biochemistry*, **42**, 4699–4708.
Xiong, Y. M., Lan, Z. D., Wang, M., Liu, B., Liu, X. Q., Fei, H., Xu, L. G., Xia, Q. C., Wang, C. G., Wang, D.-C. & Chi, C. W. (1999). *Toxicon*, **37**, 1165–1180.
Zlotkin, E., Kadouri, D., Gordon, D., Pelhate, M., Martin, M. F. & Rochat, H. (1985). *Arch. Biochem. Biophys.* **240**, 877–887.
Zlotkin, E., Rochat, H., Kopeyan, M. F. & Lissitzky, S. (1971). *Biochimie*, **53**, 1073–1078.